Optics and Lasers in Engineering 50 (2012) 869–876

Contents lists available at SciVerse ScienceDirect

Optics and Lasers in Engineering

journal homepage: www.elsevier.com/locate/optlaseng

Dynamic visual cryptography for optical control of vibration generation equipment

Vilma Petrauskiene [a], Algiment Aleksa [a], Algimantas Fedaravicius [b], Minvydas Ragulskis [a,*]

[a] Research Group for Mathematical and Numerical Analysis of Dynamical Systems, Kaunas University of Technology, Kaunas, Lithuania
[b] Institute of Defence Technologies, Kaunas University of Technology, Kaunas, Lithuania

ARTICLE INFO

Article history:
Received 4 October 2011
Received in revised form
1 December 2011
Accepted 9 January 2012
Available online 16 February 2012

Keywords:
Geometric moiré
Visual cryptography
Time-averaged fringes
Vibration control

ABSTRACT

An optical experimental technique based on dynamic visual cryptography is proposed for the optical control of vibration generation equipment. A secret image is embedded into a stochastic background using initial stochastic phase deflection and phase matching algorithms. The embedded image can be interpreted by a naked eye when the structure vibrates in the pre-determined regime; the decoding of the image is based on the formation of moiré fringes in the time-averaged image. A simple visual inspection is enough to determine if the amplitude of vibrations is kept in the tolerated range. The sensitivity of the proposed optical control method as well as the applicability of this method for different types of oscillations is discussed.

1. Introduction

Visual cryptography is a cryptographic technique which allows visual information (pictures, text, etc) to be encrypted in such a way that the decryption can be performed by the human visual system, without the aid of computers. Visual cryptography was pioneered by Naor and Shamir in 1994 [1]. They demonstrated a visual secret sharing scheme, where an image was broken up into n shares so that only someone with all n shares could decrypt the image, while any $n-1$ shares revealed no information about the original image. Each share was printed on a separate transparency, and decryption was performed by overlaying the shares. When all n shares were overlaid, the original image would appear. Since 1994, many advances in visual cryptography have been done.

Geometric moiré [2,3] is a classical in-plane whole-field non-destructive optical experimental technique based on the analysis of visual patterns produced by superposition of two regular gratings that geometrically interfere. Two basic goals exist in moiré pattern research. The first is the analysis of moiré patterns; the task is to analyze and characterize the distribution of moiré fringes in a moiré pattern. Most of the research in moiré pattern analysis deals with the interpretation of experimentally produced patterns of fringes and determination of displacements (or strains) at centerlines of appropriate moiré fringes [2].

Another goal is moiré pattern synthesis when the generation of a certain predefined moiré pattern is required. The synthesis process involves production of two such images that the required moiré pattern emerges when those images are superimposed [4]. Moiré synthesis and analysis are tightly linked and understanding one task gives insight into the other. Conditions ensuring that a desired moiré pattern will be present in the superposition of two images are predetermined; however, they do not specify these two original images uniquely. The freedom in choosing the superimposed images can be exploited to produce various degrees of visibility and ensure the desired properties. Several criteria are proposed in [5,6] to resolve that freedom in moiré pattern synthesis.

The image hiding method based on time-averaging moiré is proposed in [7]. This method is based not on static superposition of moiré images, but on time-averaging geometric moiré. This method generates only one picture; the secret image can be interpreted by the naked eye only when the original encoded image is harmonically oscillated in a predefined direction at strictly defined amplitude of oscillation. One needs a computer to encode a secret but one can decode it without a computing device. Only one picture is generated, and the secret is leaked from this picture when parameters of oscillations are appropriately tuned. In other words, the secret can be decoded by trial and error—if only one knows that he has to shake the slide. Therefore, additional image security measures are implemented in [7,8], where the secret embedded image appears

* Corresponding author at: Research Group for Mathematical and Numerical Analysis of Dynamical Systems, Kaunas University of Technology, Studentu 50-222, LT-51368 Kaunas, Lithuania. Tel.: +370 69822456; fax: +370 37330446.
E-mail addresses: vilma.petrauskiene@ktu.lt (V. Petrauskiene), algiment.aleksa@ktu.lt (A. Aleksa), algimantas.fedaravicius@ktu.lt (A. Fedaravicius), minvydas.ragulskis@ktu.lt (M. Ragulskis).
URL: http://www.personalas.ktu.lt/~mragul (M. Ragulskis).

0143-8166/$ - see front matter © 2012 Elsevier Ltd. All rights reserved.
doi:10.1016/j.optlaseng.2012.01.013

only when the encrypted image is oscillated according to a predefined law of motion; no secret is leaked when the encrypted image is oscillated harmonically. The encoding process of the secret image into stationary stochastic moiré gratings is discussed in details in [7,8]; the primary goal of these papers is to build the mathematical foundation of dynamical visual cryptography.

The object of this paper is to propose an effective optical technique for the control vibration generation equipment. In general, visual cryptography is a multidisciplinary research area of applied computer science and optical engineering. But recent modifications of visual cryptography (particularly image hiding based on time average geometric moiré) enables the development of novel optical control tools which can be exploited in different vibration related applications.

This paper is organized as follows. Initial definitions and a short overview on visual cryptography are given in Section 2; the experimental setup is discussed in Section 3; considerations about the sensitivity of the method are placed in Section 4; applicability of the technique for non-harmonic oscillations is discussed in Section 5; concluding remarks and the discussion on other potential applications of the presented technique are given in the concluding section.

2. Theoretical background

Moiré grating on the surface of a one-dimensional structure in the state of equilibrium can be interpreted as a periodic variation of black and white colors:

$$\tilde{F}(x)=\frac{1}{2}+\frac{1}{2}\sin\left(\frac{2\pi}{\lambda}x\right) \tag{1}$$

where x is the longitudinal coordinate; $\tilde{F}(x)$ is grayscale level of the surface at point x; λ is the pitch of the grating. Numerical value 0 of $\tilde{F}(x)$ corresponds to black color; 1 corresponds to white color, and all intermediate values – to appropriate grayscale levels.

Time-average geometric moiré is an optical experimental method when the moiré grating is formed on the surface of an oscillating structure and time averaging techniques are used for the registration of time averaged patterns of fringes [9]. The assumption that the deflection from the state of equilibrium varies harmonically in time:

$$u(t)=a\sin(\omega t+\varphi) \tag{2}$$

yields the one-dimensional time-averaged image [2, 7, 8]:

$$H_a(x|\tilde{F};u)=\lim_{T\to\infty}\frac{1}{T}\int_0^T\tilde{F}(x-a\sin(\omega t+\varphi))dt=\frac{1}{2}+\frac{1}{2}\sin\left(\frac{2\pi}{\lambda}x\right)J_0\left(\frac{2\pi}{\lambda}a\right) \tag{3}$$

where H_a is the time averaging operator which averages the grating $\tilde{F}(x)$ according to the deflection time function $u(t)$ [8]; ω is the cyclic frequency, φ is the phase; a is the amplitude of harmonic oscillations; T is the exposure time; J_0 is the zero order Bessel function of the first kind. Time-averaged fringes will form when $J_0((2\pi)/(\lambda)a)=0$. Thus, the relationship between the order of a time-averaged fringe, the amplitude of harmonic oscillations and the pitch of the grating takes the following form:

$$\frac{2\pi}{\lambda}a_i=r_i;\quad i=1,2,\ldots \tag{4}$$

where r_i denotes ith root of the zero order Bessel function of the first kind; a_i is the amplitude of oscillation at the center of the ith time-averaged fringe. Computationally reconstructed pattern of time-averaged fringes is presented in Fig. 1. It is assumed that $a(x)=x$; a static moiré grating is formed at $x=0$ in the interval $0\le y\le 5(\lambda=0.2)$. A clear moiré grating is visible at the left part of the time-averaged image which gets blurred and is modulated by the zero order Bessel function of the first kind as the amplitude of harmonic oscillations increases (Eq. (3)). Time-averaged fringes form around the areas where the amplitude of oscillation satisfies the relationship (4). It can be noted that the frequency of oscillations has no effect to the formation of fringes and that the exposure time must be long enough to fit in a large number of periods of oscillations.

The ability to interpret time-averaged fringes by a naked eye is exploited in developing an image encryption method based on the principles of visual cryptography and time average geometric moiré [7,8]. A secret image is embedded into the background harmonic moiré grating; the phase matching algorithm is used to eliminate discontinuities at the boundaries between the background and the secret image; the stochastic initial phase deflection algorithm is used to encrypt the secret (both algorithms are described in detail in [7]). Such an encryption method could be considered to be somewhat similar to the moiré cryptography

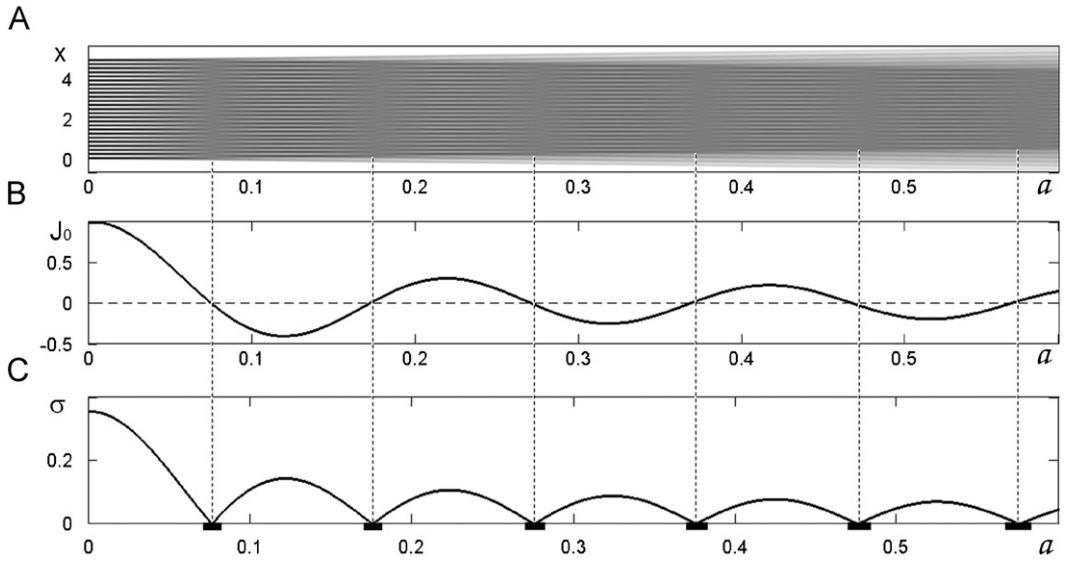

Fig. 1. Computationally reconstructed pattern of time-averaged fringes (A); the modulating zero order Bessel function of the first kind (B) and the standard deviation of the grayscale level in the time-averaged image (C); $\lambda=0.2$.

method proposed by Desmedt and Van Le [4], but there is a principal difference between optical techniques used in [4] and in [7]. Double exposure geometric moiré (a superposition of two moiré slides) is used in [4]. Time average geometric moiré is used in [7]; there are no 2 or n shares to superpose in this method. One image is used only in [7] and this image must be oscillated in a predefined direction at predefined amplitude in order to produce time-averaged moiré fringes induced by the motion blur.

It is important that the direction of harmonic oscillations used to decode the secret must coincide with the direction perpendicular to the constitutive moiré grating lines used to encode the secret. Theoretically, the time of exposure should tend to infinity (we do not use stroboscopic illumination to cut out a single period of oscillations). In practice, it is enough that a large number of periods of oscillation would fit into the time of exposure [2,10]. As shown previously, the frequency of oscillations does not have any influence to the formation of the time-averaged image (Eq. (3)). Nevertheless, one must use a sufficiently high frequency of oscillations allowing the naked eye to average fast dynamical processes.

Fig. 2. The general view of the experimental setup.

3. The experimental setup

As mentioned previously, the decoding method of the secret image is based on the optical time averaging of the encoded oscillating image. This image can be fixed onto the surface of a solid non-deformable body which performs periodic oscillations. The experimental setup used for the implementation of this visualization technique comprises a shaker table and an ordinary optical camera (Fig. 2). The encoded image is printed by an ordinary digital printer and glued onto the surface of a rigid structure which is fixed to the head of the shaker table. It is important to check that this rigid structure (and the fixture in whole) would not possess structural resonances at the pre-determined range of excitation frequencies – the visual decoding procedure is based on in-plane periodic oscillations.

As mentioned previously, theoretical results show that the frequency of oscillations does not have any influence to the formation of time-averaged fringes. Nevertheless, the frequency must be high enough if the decoding is visual and performed by a naked eye. On the other hand, the exposure time must be long enough to accommodate a sufficient number of periods of oscillations if the time-averaged image is to be acquired by a photographic camera (analog or digital).

The concept of the standard deviation of the grayscale level in a time-averaged image $\sigma(H_a\tilde{F}(x))$ is introduced in [11] in order to quantify the development of a time-averaged fringe. The standard deviation of a time-averaged image can be also used to quantity errors induced by a finite exposure time. Let us assume that the amplitude is set to a value ensuring the formation of the first time-averaged fringe: $a_1 = r_1(\lambda)/(2\pi)$. Then Eq. (3) yields the identity $H_{a_1}(x|\tilde{F};u) = 0.5$ where $\tilde{F}(x)$ is defined by Eq. (1) and the exposure time tends to infinity. Instead we calculate a definite integral $(1/T)\int_0^T \tilde{F}(x - a_1\sin(\omega t + \varphi))dt$ and plot the results for different values of T in Fig. 3. It is clear that the error introduced by a finite exposure time diminishes within a range of few percents

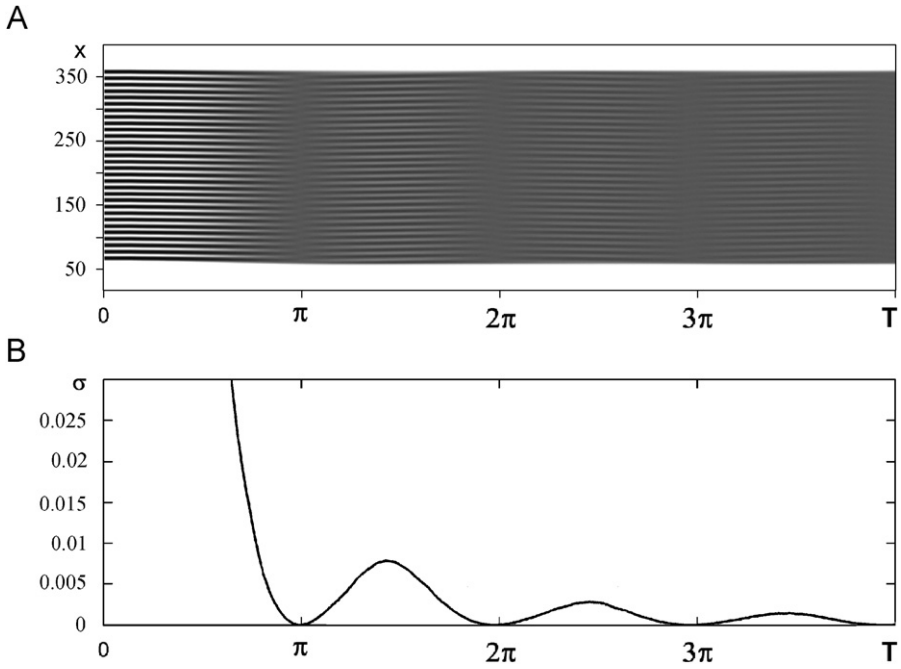

Fig. 3. The development of the time-averaged fringe (A) and the standard deviation of the grayscale level (B) as the exposure time increases.

(what is completely acceptable for visual interpretation of time-averaged fringes) as T becomes longer than 10 periods of harmonic oscillation.

We select the frequency of oscillations $\omega=60$ Hz and the time of exposure $T=1/15$ s. Thus, around 4 periods of oscillations fit into the time of exposure. If some fractional part of the period is cut out at the beginning or at the end of the exposure interval, that has a small effect to the process of time averaging.

The secret image is shown in Fig. 4(A); the encrypted image in harmonic moiré background is shown in Fig. 4(B); the computationally decrypted image is shown in Fig. 4(C) (the encrypted image is deflected from the state of equilibrium according to a harmonic law $u(t)$). Time-averaged moiré fringes are clearly seen in the regions occupied by the secret image (Fig. 4(C)); computational enhancement of the contrast helps to highlight the secret in the time-averaged image (Fig. 4(D)).

The printed encrypted image fixed to the head of the shaker table is shown in Fig. 5; the pitch of the moiré grating used for the background is 0.2292 mm; the pitch of the moiré grating in the regions of the secret image is 0.2645 mm. Time-averaged images when the amplitude of harmonic oscillations is set to $a=0.1012$ mm ($J_0((2\pi)/(0.2645)0.1012)=J_0(r_1)=0$) and $a=0.0877$ mm ($J_0((2\pi)/(0.2292)0.0877)=J_0(r_1)=0$) are shown in Figs. 6 and 7; the secret image is clearly interpretable in both images by a naked eye. By the way, it can be noted that images interpreted by a naked eye are better than recorded by the digital camera (due to comparatively short exposure times). A slight mismatch of the amplitude ($a=0.0938$ mm) prevents visual decoding of the secret image – no time-averaged fringes can be observed in Fig. 8.

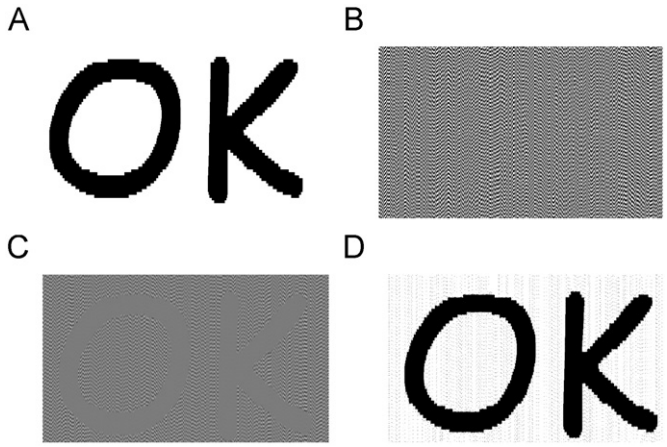

Fig. 4. The secret image (A); the secret image encoded into the moiré background (B); computational decryption of the secret (C) and contrast enhancement of the decrypted image (D).

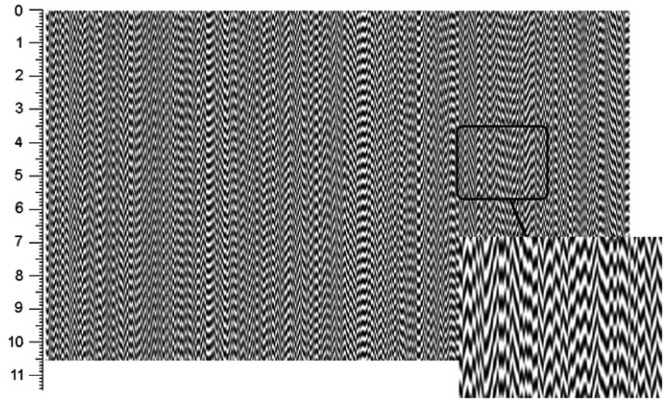

Fig. 5. The photo of the encoded image (the optically zoomed part shows the structure of the moiré grating in the printed image).

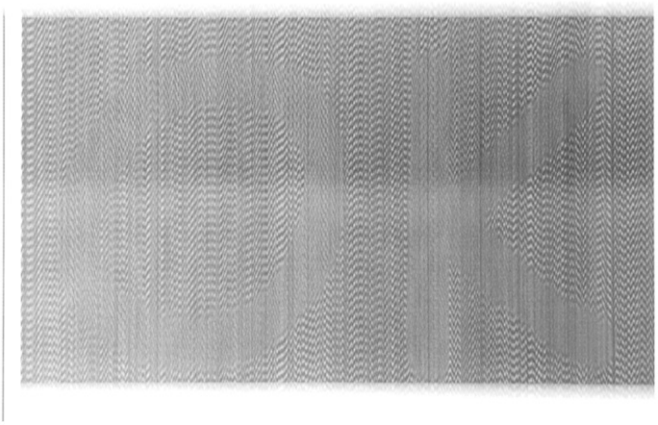

Fig. 6. Time-averaged image of the oscillating structure; time-averaged fringes form the symbol "OK".

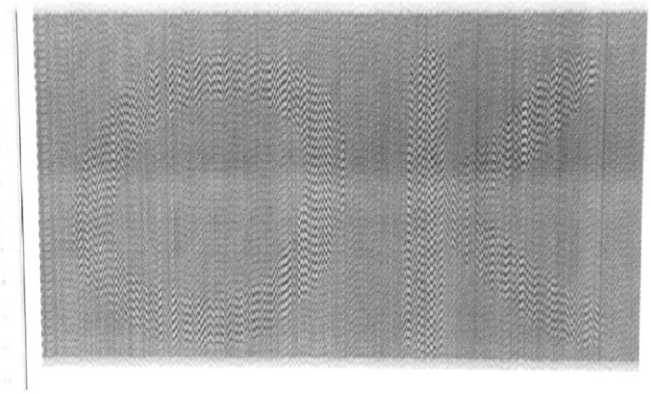

Fig. 7. Time-averaged image; time-averaged fringes form in the background.

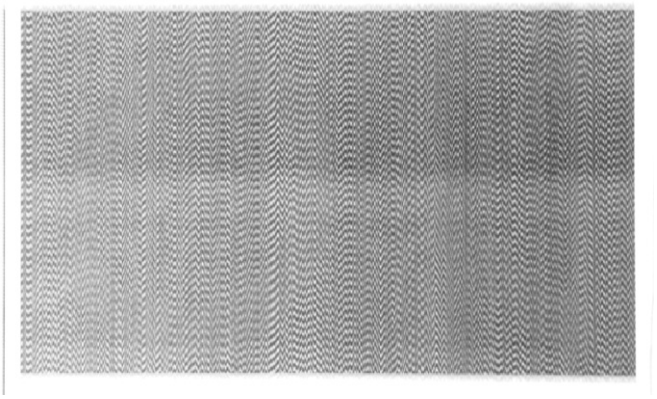

Fig. 8. Incorrect amplitude of harmonic oscillations prevents visual decoding of the secret.

4. Considerations about the sensitivity of the method

It is clear that the sensitivity of the proposed method is determined by pitches of moiré gratings used to represent the background and the secret image. Let us assume that the pitch at the background is λ_0 and the pitch at the region inherent to the

secret image is λ_1 (we consider the most simple case when only one secret image is encoded into the background moiré grating). Initially, let us consider harmonic oscillations. Then, time-averaged fringes will form at the background when the encoded image is oscillated harmonically and the amplitude of these oscillations is equal to one of the discreet values:

$$a_j = r_j \frac{\lambda_0}{2\pi}; \quad j = 1,2,\ldots \tag{5}$$

Analogously, time averaged fringes will form at the region inherent to the secret image when the amplitude of harmonic oscillations is

$$b_j = r_j \frac{\lambda_0}{2\pi}; \quad j = 1,2,\ldots \tag{6}$$

The highest possible resolution of the proposed technique (in the amplitude domain) could be achieved when λ_1 is almost equal to λ_0, but we will not consider such extremes because the optical interpretation of the secret image would become problematic then. Instead, we consider the opposite situation when λ_1 is located as far as possible from λ_0 and its recurrent values (contrast differences of the background and the secret image are highest then). As mentioned previously, roots of the zero order Bessel function of the first kind are not periodic. Nevertheless, if b_1 can be placed exactly in the middle of the interval $[a_1;a_2]$. Then $b_1 = 0.5(a_1+a_2)$, what yields:

$$\lambda_1 = \frac{r_1+r_2}{r_1}\lambda_0. \tag{7}$$

In other words, the effective step of the amplitude Δa (when the location of time-averaged fringes switches between the background and the secret) is:

$$\Delta a \approx b_1 - a_1 = \frac{r_2}{2\pi}\lambda_0 \approx 0.878\lambda_0. \tag{8}$$

Ordinary digital printing techniques enable printing a high quality moiré grating comprising up to 2 lines per millimeter (much higher densities can be achieved with specialized printing equipment and surface coatings). Thus, it is rather easy to achieve that Δa is lower than 0.5 mm.

But one has to have in mind that the proposed technique is based on the principle of visual cryptography. In other words, one must accurately tune the amplitude of oscillations in order to decrypt the secret (undeveloped time-averaged fringes prevent visual decryption). The relationship between the amplitude of harmonic oscillations and the standard deviation of the grayscale level in a time-averaged image (for a harmonic moiré grating) reads [11] (Fig. 1(C)):

$$\sigma(H_a(x|\tilde{F};u)) = \frac{|J_0((2\pi/\lambda)a)|}{\sqrt{8}}. \tag{9}$$

The secret image is interpretable if the standard deviation is not higher than 0.01 (a dashed line in Fig. 1(C)). Then, regions of amplitudes ensuring visual decryption of the secret are marked as thick solid intervals on the a-axis in Fig. 1(C). The width of the interval around the first root of the zero order Bessel function of the first kind is about 10 times smaller than Δa (Fig. 1(C)). Thus, an easily achievable sensitivity of the method is 0.05 mm. In other words, the proposed optical control technique can discriminate a change of the amplitude of oscillations larger than 0.05 mm. Note that this can be achieved using an ordinary digital printer without special printing surface preparation techniques. Of course, the sensitivity can be decreased (if necessary) by enlarging pitches of moiré gratings used to encrypt the secret image.

5. Non-harmonic oscillations

As mentioned previously, the security of the encryption can be increased by applying special image formation techniques which allow visual decryption only when the encrypted image is oscillated according to a predefined law of motion [8] and stepped periodic moiré gratings are used instead of harmonic moiré gratings.

Let us assume that the moiré grating $\overline{F}(x)$ is a stepped periodic function – the grating is formed as the array of white and dark bands:

$$\overline{F}(x) = \begin{cases} 1, & \text{when } x \in [\lambda j;\ \lambda(j+0.5)]; \\ 0, & \text{when } x \in (\lambda(j+0.5);\ \lambda(j+1)); \end{cases} \quad j \in Z; \tag{10}$$

where λ is the pitch of the stepped moiré grating. The Fourier expansion of Eq. (10) reads:

$$\overline{F}(x) = \frac{\alpha_0}{2} + \sum_{k=1}^{\infty}\left(\alpha_k \cos\frac{2\pi kx}{\lambda} + \beta_k \sin\frac{2\pi kx}{\lambda}\right); \tag{11}$$

where

$$\alpha_0 = 1; \quad \alpha_1,\alpha_2,\alpha_3,\ldots = 0; \quad \beta_k = \frac{1+(-1)^{k+1}}{k\pi}; \quad k = 1,2,\ldots. \tag{12}$$

Now, harmonic oscillations yield [8]:

$$H_a(x|\overline{F};u) = \frac{1}{2} + \sum_{k=1}^{\infty}\left(\frac{1+(-1)^{k+1}}{k\pi}\sin\frac{2\pi kx}{\lambda}\right)J_0\left(\frac{2\pi k}{\lambda}a\right); \tag{13}$$

what does not produce fully developed time-averaged fringes due to the reason that roots of the zero order Bessel function of the first kind are not periodic. Now, let us assume that the function describing the deflection from the state of equilibrium is not a harmonic but a triangular waveform function $z(t)$ instead (the maximum deflection from the state of equilibrium a and the frequency of oscillations ω are still the same as for $u(t)$ defined in Eq. (2)):

$$z(t) = \begin{cases} \frac{2a\omega}{\pi}\left(t - \left(\frac{2\pi}{\omega}j - \frac{\pi}{2\omega}\right)\right) - a & \text{when} \left(\frac{2\pi}{\omega}j - \frac{\pi}{2\omega}\right) \le t < \left(\frac{2\pi}{\omega}j + \frac{\pi}{2\omega}\right); \\ -\frac{2a\omega}{\pi}\left(t - \left(\frac{2\pi}{\omega}j + \frac{\pi}{2\omega}\right)\right) + a & \text{when} \left(\frac{2\pi}{\omega}j + \frac{\pi}{2\omega}\right) \le t < \left(\frac{2\pi}{\omega}j + \frac{3\pi}{2\omega}\right); \end{cases} \quad j \in Z. \tag{14}$$

Then, according to [8],

$$H_a(x|\overline{F};z) = \frac{1}{2} + \sum_{k=1}^{\infty}\left(\frac{1+(-1)^{k+1}}{k\pi}\sin\frac{2\pi kx}{\lambda}\right)\frac{\sin((2\pi k/\lambda)a)}{((2\pi k/\lambda)a)}$$

what guarantees full development of time-averaged fringes because roots of the characteristic function $\sin(y)/y$ are periodic.

The experimental setup for visual decoding of the secret image by triangular waveform type oscillations is analogous to the previously described setup based on harmonic oscillations. Nevertheless, there is one important difference. The relationship between the order of a time-averaged fringe, the amplitude of triangular waveform type oscillations and the pitch of the grating takes the following form now:

$$a_k = \frac{\lambda}{2}k; \quad k = 1,2,\ldots; \tag{15}$$

the distribution of roots of characteristic functions $J_0((2\pi)/(\lambda)a)$ and $\sin(2\pi/\lambda)a/(2\pi/\lambda)a$ are shown in Fig. 9.

We repeat computational experiments with the secret image, but it is now embedded in the stepped moire grating (Fig. 10). The printed encrypted image fixed to the head of the shaker table is shown in Fig. 11 (the fact that stepped moiré gratings are used instead of harmonic gratings can be clearly seen in the inset); the pitch of the moiré grating used for the background is 0.2821 mm; the pitch of the moiré grating in the regions of the secret image is 0.3174 mm. Time-averaged images when the amplitude of triangular waveform type oscillations is set to $a = 0.14105$ mm $(\sin((2\pi/0.2821)0.14105) = \sin(\pi) = 0)$ are shown in Fig. 12; the secret image is clearly interpretable by a naked eye. The secret

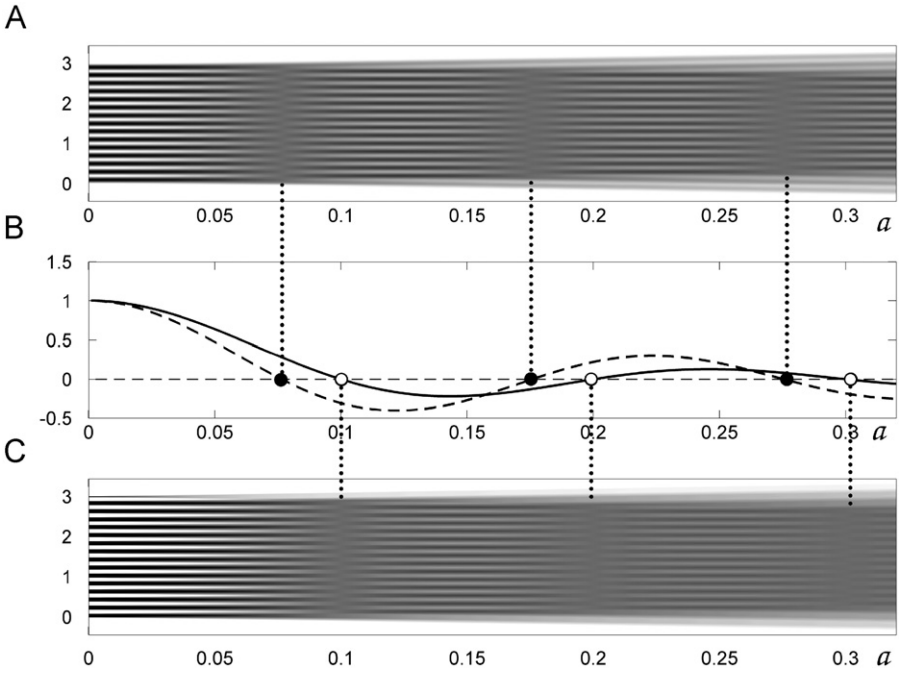

Fig. 9. Computationally reconstructed pattern of time-averaged fringes formed by a harmonic moire grating (A); computationally reconstructed pattern of time-averaged fringes formed by a stepped moire grating (C); the modulating function $J_0((2\pi)/(\lambda)a)$ (the dashed line) and the modulating function $\sin(2\pi/\lambda)a/(2\pi/\lambda)a$ (the solid line) are shown in part (B); pitches of both gratings are equal to $\lambda=0.2$.

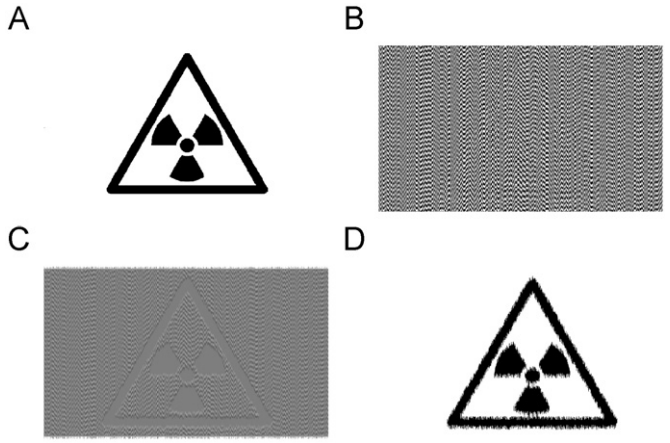

Fig. 10. The secret image (A); the secret image encoded into the moiré background (B); computational decryption of the secret (C) and contrast enhancement of the decrypted image (D).

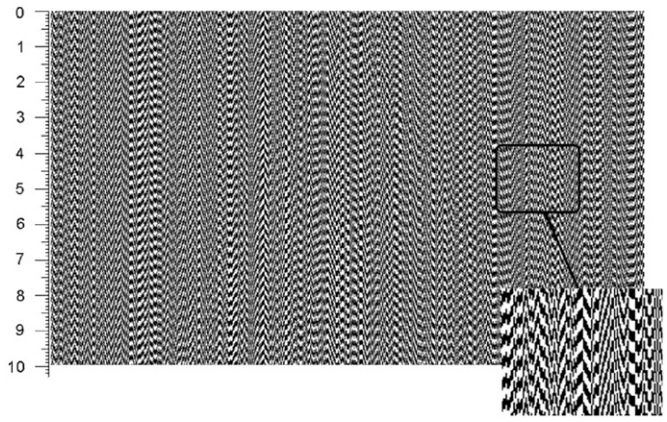

Fig. 11. The secret image encoded into a stepped moiré grating (the optically zoomed part reveals the structure of the moiré grating).

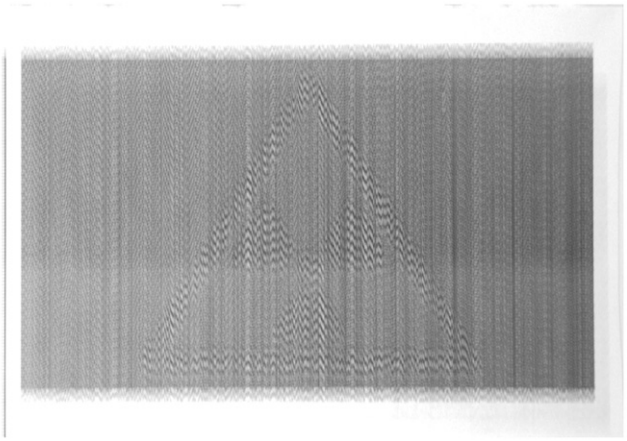

Fig. 12. Time-averaged fringes form in the background and reveal the secret embedded into a stepped moiré grating.

cannot be decoded using harmonic oscillations. No time-averaged fringes develop when the amplitude of harmonic oscillations is set to 0.1080 mm (though $J_0((2\pi)/(0.2821)0.1080)=J_0(r_1)=0$); the optical image is presented in Fig. 13.

6. The sensitivity of the proposed method to phase jitter

Another important aspect of the proposed method is its sensitivity to phase jitter, even if average frequency (rpm) is strictly constant. Jitter is a statistical measure of noisy oscillation process when the period of each cycle is different due to the noise-induced jitter [12,13]. The phase noise can be characterized by the cycle jitter σ_c^2 [14]. It measures the variance of each period to the average period of oscillations:

$$\sigma_c^2=\lim_{N\to\infty}\left(\frac{1}{N}\sum_{n=1}^{N}(\tau_n-\tau_{avg})^2\right); \tag{16}$$

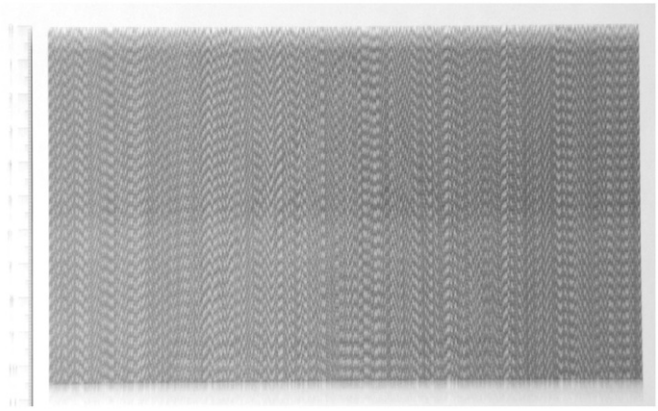

Fig. 13. The secret cannot be leaked at any amplitude of harmonic oscillations.

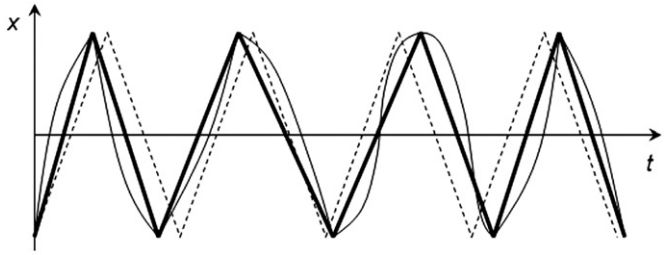

Fig. 14. Phase jitter in triangular waveform oscillations. The dashed line shows stationary oscillations without phase jitter; thick solid lines stand for triangular waveform oscillations with phase jitter; thin solid lines illustrate the jitter in the waveform itself.

where N is the number of periods; τ_n is the length of the n-th period; τ_{avg} is the average length of all periods (the average frequency of oscillations is $1/(\tau_{\text{avg}})$.

Without loosing the generality we will consider triangular waveform type oscillations with phase jitter (Fig. 14). The dashed line shows stationary oscillations without phase jitter; thick solid lines stand for triangular waveform oscillations with phase jitter; thin solid lines illustrate the jitter in the waveform itself.

As mentioned previously, the formation of time-averaged moiré fringes is governed by the time function describing the deflection from the state of equilibrium. Let us assume that the Fourier expansion of the moiré grating is defined by Eq. (11) and the density function of the waveform $w(t)$ is $p_a(x)$. Moreover (in addition to other standard properties of density functions), we require that the function $p_a(x)$ is even and that $p_a(x)=0$ when $x<-a$ and $x\ a$. Then, the time averaged image takes the form [8]:

$$H_a(x|F;w)=\frac{\alpha_0}{2}+\sum_{k=1}^{\infty}\left(\alpha_k\cos\frac{2\pi kx}{\lambda}+\beta_k\sin\frac{2\pi kx}{\lambda}\right)\Phi\left(\frac{2\pi k}{\lambda}a\right); \quad (17)$$

where the symbol Φ stands for the Fourier transform of $p_a(x)$. This theoretical result yields an important conclusion that the proposed method is not sensitive to the phase jitter. In other words, the density function of the time process denoted by the thick solid line and the density function of the time process denoted by the dashed line in Fig. 14 are the same – it can be described as the density of a random variable distributed uniformly in the interval $[-a;a]$ (Fourier transform of this density function is $\sin(2\pi/\lambda)a/(2\pi/\lambda)a$ [8]).

But the situation becomes much more complex if the waveform itself is deformed due to the jitter (the thin solid line in Fig. 14). Then one should consider the question what happens when oscillations are chaotic. These questions are investigated in detail in [15] and fall out of scope of interests for this paper.

7. Concluding remarks

So far the applicability of dynamic visual cryptography has been investigated for stationary vibrations only. It has been shown that the functionality of the system does not depend on the frequency of oscillations (though the frequency must be high enough to accommodate a considerable number of periods of oscillation in the exposure time). Thus, in principle, the proposed technique could be also applied for optical control of transient oscillations – if only the amplitude of these oscillations is kept constant. Such situations may occur during the run-up of a turbine, for example, when the frequency of the rotation gradually increases. The main factors determining the formation of time-averaged moiré fringes are the amplitude of oscillations and the waveform determining the shape of the signal. The proposed system would work well if the amplitude of oscillations would be kept constant in the run-up process. Otherwise, the fringe formation process becomes much more complex and such situations are left for the future research.

It can be noted that we have examined uni-directional vibrations only. It is quite common that vibrations (even harmonic) can be elliptic. In general, the proposed technique would work well in case of elliptic vibrations also. It is well known that a stationary geometric moiré grating comprised from an array of parallel lines is not sensitive to planar displacements along the constitutive grating lines. Nevertheless, experimental investigation of elliptic (and also 2D chaotic in-plane vibrations) is also left for the future research.

Two different waveforms have been investigated in this paper – harmonic and triangular waveforms. In principle, the proposed method is applicable for any periodic waveform. One would need to compute the density function corresponding to the given waveform and to derive its Fourier transform. Thus, for example stepped-type oscillations (when the system stays for the longest periods of times at the positions of maximal deflections from the state of equilibrium) could be also successfully controlled.

The basic idea of the proposed optical control technique is based on the fact that sophisticated computational tools are required to encode the secret image, but the decoding process is completely visual. In other words, the decoding process is based on the inability of human visual system to track fast moving objects. The eyes start averaging (blurring) the oscillating image. The eye is connected to the brain, a massive pattern recognition machine, where the time averaged moiré fringes can be directly interpreted as the secret decoded image. On the other hand, that sets the lower boundary in terms of the frequency of oscillation to the applicability of the proposed method. If the frequency of oscillation would be low enough (for example, 0.5 Hz) the eye would track the cover image and no patterns would be formed in the brain (though mathematical relationships guarantee that the frequency does not play any role in the formation of time-averaged fringes).

Some experimental images may look not very clear. Note that we do not expect a time-averaged moiré fringe to be fully developed. Otherwise, the applicability of the proposed method would be rather questionable – the amplitude of the oscillation should be strictly set to an infinitesimally accurate value. Instead, we set a maximal limit for the standard deviation of the grayscale level – when a time-averaged fringe can be considered as an almost developed one. This maximal level of the standard deviation is related to the ability to differentiate between the background and the secret image. Therefore, secret images in experimental photos may look not ideally evenly gray, though the shape of the secret picture is clearly interpretable. This level of the standard deviation is directly related to the properties of the human visual system discussed above.

A simple optical control technique for the control of vibrating equipment is proposed in this paper. The secret image embedded into a stochastic moiré background can be observed by a naked eye

when the amplitude of vibration fits into a predetermined range of values. Such a control technique can be advantageous in particular industrial or technological environments (a laboratory shaker table for precise mixing of fluid suspensions could be a typical example). One could print an encoded image and stick it to the surface of the vibrating structure. The secret image must be encoded in such a way that the secret would leak when the structure vibrates in the predetermined regime only. That secret information could be just two letters "OK", for example. A simple visual inspection could be enough to determine if the amplitude of vibrations is kept in the tolerated range. This is a completely zero energy optical control method. Moreover, it is functional in any transparent environment (in vacuum or in fluids). An application of this control technique in different set-ups, especially for non-stationary vibrations, is a definite object of future research.

Acknowledgments

Financial support from the Lithuanian Science Council under project No. MIP-041/2011 is acknowledged.

References

[1] Naor M, Shamir A. Visual cryptography. EUROCRYPT 1994:1–12.
[2] Kobayashi AS. Handbook on Experimental Mechanics. 2nd ed. Bethel, CT: SEM; 1993.
[3] Patorski K, Kujawinska M. Handbook of the Moiré Fringe Technique. Amsterdam: Elsevier; 1993.
[4] Desmedt Y, Van Le T. Moiré cryptography. 7th ACM Conf. Comput. Commun. Secur. 2000:116–24.
[5] Lebanon G, Bruckstein AM. A variational approach to moiré pattern synthesis. J. Opt. Soc. Am. A: 2001;18(6):1371–81.
[6] Lebanon G, Bruckstein AM. On designing moiré patterns. Lect. Notes Comput. Sci. 2001;2134:185–201.
[7] Ragulskis M, Aleksa A. Image hiding based on time-averaging moiré. Opt. Commun. 2009;282(14):2752–9.
[8] Ragulskis M, Aleksa A, Navickas Z. Image hiding based on time-averaged fringes produced by non-harmonic oscillations. J. Opt. A: Pure Appl. Opt. 2009;11(12):125411.
[9] Liang CY, Hung YY, Durelli AJ, Hovanesian JD. Time-averaged moiré method for in-plane vibrational analysis. J. Sound Vib. 1979;62(2):267–75.
[10] Ragulskis M, Maskeliunas R, Ragulskis L, Turla V. Investigation of dynamic displacements of lithographic press rubber roller by time average geometric moiré. Opt. Lasers Eng. 2005;43(9):951–62.
[11] Ragulskis M, Saunoriene L, Maskeliunas R. The structure of moiré grating lines and influence to time averaged fringes. Exp. Tech. 2009;33(2):60–4.
[12] Demir A, Mehrotra A, Roychowdhury J. Phase noise in oscillators: a unifying theory and numerical methods for characterization. IEEE Trans. Circuits Syst. 2000;47:655–74.
[13] Herzel F, Razavi B. A study of oscillator jitter due to supply and substrate noise. IEEE Trans. Circuits Syst. 1999;46:56–62.
[14] Hajimiri A, Limotyrakis S, Lee TH. Jitter and phase noise in ring oscillators. IEEE J. Solid-State Circuits 1999;34:790–804.
[15] Ragulskis M, Sanjuan MAF, Saunoriene L. Applicability of time average moiré techniques for chaotic oscillations. Phys. Rev. E 2007;76. Art. no. 036208.